Physics Letters B 792 (2019) 263–268

Contents lists available at ScienceDirect

Physics Letters B

www.elsevier.com/locate/physletb

New isomers in $^{125}Pd_{79}$ and $^{127}Pd_{81}$: Competing proton and neutron excitations in neutron-rich palladium nuclides towards the $N = 82$ shell closure

H. Watanabe [a,b,c,*], H.K. Wang [d], G. Lorusso [c], S. Nishimura [c], Z.Y. Xu [f], T. Sumikama [g], P.-A. Söderström [c], P. Doornenbal [c], F. Browne [c,h], G. Gey [c,i], H.S. Jung [j], J. Taprogge [c,k,l], Zs. Vajta [c,m], J. Wu [c,n], A. Yagi [o], H. Baba [c], G. Benzoni [p], K.Y. Chae [q], F.C.L. Crespi [p,r], N. Fukuda [c], R. Gernhäuser [s], N. Inabe [c], T. Isobe [c], A. Jungclaus [l], D. Kameda [c], G.D. Kim [t], Y.K. Kim [t,u], I. Kojouharov [v], F.G. Kondev [w], T. Kubo [c], N. Kurz [v], Y.K. Kwon [t], G.J. Lane [x], Z. Li [n], C.-B. Moon [y], A. Montaner-Pizá [z], K. Moschner [aa], F. Naqvi [ab], M. Niikura [f], H. Nishibata [o], D. Nishimura [ac], A. Odahara [o], R. Orlandi [ad], Z. Patel [e], Zs. Podolyák [e], H. Sakurai [c], H. Schaffner [v], G.S. Simpson [i], K. Steiger [s], Y. Sun [ae,af], H. Suzuki [c], H. Takeda [c], A. Wendt [aa], K. Yoshinaga [ag]

[a] School of Physics and Nuclear Energy Engineering, Beihang University, Beijing 100191, China
[b] International Research Center for Nuclei and Particles in the Cosmos, Beihang University, Beijing 100191, China
[c] RIKEN Nishina Center, 2-1 Hirosawa, Wako, Saitama 351-0198, Japan
[d] College of Physics and Telecommunication Engineering, Zhoukou Normal University, Henan 466000, China
[e] Department of Physics, University of Surrey, Guildford GU2 7XH, United Kingdom
[f] Department of Physics, University of Tokyo, Hongo, Bunkyo-ku, Tokyo 113-0033, Japan
[g] Department of Physics, Tohoku University, Aoba, Sendai, Miyagi 980-8578, Japan
[h] School of Computing, Engineering and Mathematics, University of Brighton, Brighton, BN2 4GJ, United Kingdom
[i] LPSC, Université Joseph Fourier Grenoble 1, CNRS/IN2P3, Institut National Polytechnique de Grenoble, F-38026 Grenoble Cedex, France
[j] Department of Physics, Chung-Ang University, Seoul 156-756, Republic of Korea
[k] Departamento de Física Teórica, Universidad Autónoma de Madrid, E-28049 Madrid, Spain
[l] Instituto de Estructura de la Materia, CSIC, E-28006 Madrid, Spain
[m] MTA Atomki, O. Box 51, Debrecen, H-4001, Hungary
[n] School of Physics and State Key Laboratory of Nuclear Physics and Technology, Peking University, Beijing 100871, China
[o] Department of Physics, Osaka University, Machikaneyama-machi 1-1, Osaka 560-0043 Toyonaka, Japan
[p] INFN, Sezione di Milano, via Celoria 16, I-20133 Milano, Italy
[q] Department of Physics, Sungkyunkwan University, Suwon 440-746, Republic of Korea
[r] Dipartimento di Fisica, Universitá di Milano, via Celoria 16, I-20133 Milano, Italy
[s] Physik Department, Technische Universität München, D-85748 Garching, Germany
[t] Rare Isotope Science Project, Institute for Basic Science, Daejeon 305-811, Republic of Korea
[u] Department of Nuclear Engineering, Hanyang University, Seoul 133-791, Republic of Korea
[v] GSI Helmholtzzentrum für Schwerionenforschung GmbH, 64291 Darmstadt, Germany
[w] Physics Division, Argonne National Laboratory, Argonne, IL 60439, USA
[x] Department of Nuclear Physics, R.S.P.E., Australian National University, Canberra, A.C.T 2601, Australia
[y] Department of Display Engineering, Hoseo University, Chung-Nam 336-795, Republic of Korea
[z] IFIC, CSIC-Universidad de Valencia, A.C. 22085, E 46071, Valencia, Spain
[aa] Institut für Kernphysik, Universität zu Köln, Zülpicher Strasse 77, D-50937 Köln, Germany
[ab] Wright Nuclear Structure Laboratory, Yale University, New Haven, CT 06520-8120, USA
[ac] Department of Physics, Tokyo City University, Setagaya-ku, Tokyo 158-8557, Japan
[ad] Instituut voor Kern en Stralingsfysica, KU Leuven, University of Leuven, B-3001 Leuven, Belgium
[ae] School of Physics and Astronomy, Shanghai Jiao Tong University, Shanghai 200240, China
[af] Collaborative Innovation Center of IFSA, Shanghai Jiao Tong University, Shanghai 200240, China
[ag] Department of Physics, Faculty of Science and Technology, Tokyo University of Science, 2641 Yamazaki, Noda, Chiba, Japan

* Corresponding author at: School of Physics and Nuclear Energy Engineering, Beihang University, Beijing 100191, China.
E-mail address: hiroshi@ribf.riken.jp (H. Watanabe).

https://doi.org/10.1016/j.physletb.2019.03.053

ARTICLE INFO

Article history:
Received 6 February 2019
Received in revised form 28 February 2019
Accepted 26 March 2019
Available online 1 April 2019
Editor: D.F. Geesaman

ABSTRACT

The neutron-rich isotopes of palladium have attracted considerable interest in terms of the evolution of the $N = 82$ neutron shell closure and its influence on the *r*-process nucleosynthesis. In this Letter, we present the first spectroscopic information on the excited states in $^{125}Pd_{79}$ and $^{127}Pd_{81}$ studied using the EURICA γ-ray spectrometer, following production via in-flight fission of a high-intensity ^{238}U beam at the RIBF facility. New isomeric states with half-lives of 144(4) ns and 39(6) μs have been assigned spins and parities of $(23/2^+)$ and $(19/2^+)$ in ^{125}Pd and ^{127}Pd, respectively. The observed level properties are compared to a shell-model calculation, suggesting the competition between proton excitations and neutron excitations in the proton-hole and neutron-hole systems in the vicinity of the doubly magic nucleus ^{132}Sn.

Atomic nuclei are self-bound, quantum many-body systems consisting of two types of constituents (nucleons), protons and neutrons, which interact strongly with each other in a finite volume. The protons and neutrons respectively occupy their single-particle orbits in a mean-field potential, giving rise to a distinct pattern of the energy spacing between the orbits, so-called shell structure. In a shell-model approach, individual energy/spin eigenstates are described as the combination of proton and neutron configurations formed within the available model space assuming a doubly closed-shell nucleus as an inert core; therefore, a main difficulty is ascribed to an increasing number of configurations that have to be dealt with in the calculation, when increasing the proton/neutron valency moving away from the closed shells. Nowadays, the shell structures are known to be changed with the variation of the proton or neutron number, as well as with specific particle-hole excitations within the same nucleus, due predominantly to the monopole part of the proton-neutron interaction that includes the central and tensor forces [1,2]. Such a shell evolutionary behavior is expected to become pronounced when the proton-neutron imbalance is very large, leading to lost or new magic numbers (see, for instance, Ref. [3] and references therein). As such, spectroscopic studies of short-lived rare isotopes (exotic nuclides) around proton/neutron shell closures are of crucial significance in corroborating the shell evolution far off stability. The available spectroscopic data of excitation spectra can serve as a good testing ground for developing nuclear shell models.

The advent of the new generation in-flight-separator facility, the RI-Beam Factory (RIBF) in RIKEN Nishina Center [4], has enabled us to explore previously inaccessible nuclear regions with a highly unbalanced ratio of neutrons to protons [5]. Concerning neutron-rich palladium ($_{46}$Pd) isotopes, those with $A = 125 - 131$ ($N = 79 - 85$) have been identified as new isotopes at RIBF [6–8], followed by spectroscopic studies by means of β- and isomeric-decay measurements [9–11] and in-beam γ-ray spectroscopy [12] in the last decade. Especially emphasized is that the delayed γ-ray measurements following isomeric decays can provide a powerful tool for investigating the excited level structure, in particular, when the nucleus of interest lies at the boundaries of availability for spectroscopic studies. For $^{128}Pd_{82}$, which is a presumed waiting-point nucleus that contributes significantly to the formation of the second peak in the *r*-process solar abundance distribution [13,14], a seniority isomer with a spin and parity of (8^+) had been identified, serving as an indirect evidence for the robustness of the $N = 82$ shell closure [10]. In the two-neutron-hole neighbor $^{126}Pd_{80}$, it turned out that the proton-neutron monopole properties of the central and tensor forces play an important role in the emergence of the long-lived (10^+) isomer [11]. Compared to such even-even systems, neighboring odd-mass nuclei exhibit more complicated excitation spectra, which provide crucial information on the effect of unpaired nucleons on the level structure. This Letter presents previously unreported isomeric states and their decay properties in $^{125}Pd_{79}$ and $^{127}Pd_{81}$, which have three and one neutron holes relative to the $N = 82$ shell closure, respectively. The obtained results are compared to a shell-model calculation, which predicts the competition between proton and neutron excitations in the proton-hole and neutron-hole systems in the south-west quadrant of the doubly magic nucleus ^{132}Sn.

The neutron-rich odd-*A* palladium isotopes, ^{125}Pd and ^{127}Pd, were separated through the BigRIPS in-flight separator [15], following production via in-flight fission of a $^{238}U^{86+}$ beam at 345 MeV/u incident on a beryllium target with a thickness of 3 mm. The primary beam intensity ranged from 7 to 12 pnA during the experiments. About 3.1×10^5 ($^{125}Pd^{46+}$) and 8.7×10^3 ($^{127}Pd^{46+}$) ions were transported through the BigRIPS-ZeroDegree spectrometer and finally implanted into the WAS3ABi active stopper, which consisted of eight layers of double-sided silicon-strip detectors (DSSSDs) stacked compactly [16]. Each DSSSD had a thickness of 1 mm with an active area segmented into sixty and forty strips (1-mm pitch) on each side in the horizontal and vertical dimensions, respectively. Gamma rays emitted following the heavy-ion implantation and their subsequent radioactive decay were detected by the EURICA γ-ray spectrometer [16,17], consisting of 12 Cluster-type detectors, each of which contained seven HPGe crystals packed closely. The methodology of how to analyze the experimental data taken with the EURICA setup is described in detail in a recent review article [18].

Since ^{125}Pd and ^{127}Pd were discovered as new isotopes at RIBF [6,7], their spectroscopic information has so far been limited only to the ground-state β-decay half-lives [9]. In the present work, γ rays emitted from the excited states in these neutron-rich odd-*A* nuclei have been observed for the first time. Detailed experimental results of each isotope are described as follows:

For ^{125}Pd, four γ rays at energies of 108, 115, 757, and 825 keV are clearly visible within a time interval of $250 - 1250$ ns after the ion implantation, as exhibited in Fig. 1(a). They are unambiguously assigned as the transitions forming a single cascade from an isomeric state, which can be confirmed by their mutual coincidence as demonstrated in Fig. 1(b), as well as by their consistent time behavior as summarized in the last column of Table 1. An example of the time spectrum obtained with a gate on the 757-keV γ ray is shown in Fig. 2(a). A weighted average of the respective fits to the decay curves results in an isomeric half-life of 144(4) ns.

According to the β-decay studies of ^{125}Pd [21] carried out in parallel with the present analysis, there are two β-decaying states with similar half-lives, as systematically found in neutron-rich odd-*A* isotopes of $_{50}$Sn and $_{48}$Cd with $N \lesssim 82$ [23,24]. Either a spin-parity of $11/2^-$ or $3/2^+$ is assigned for the β-decaying isomer, and the counterpart for the ground state. The β decay from

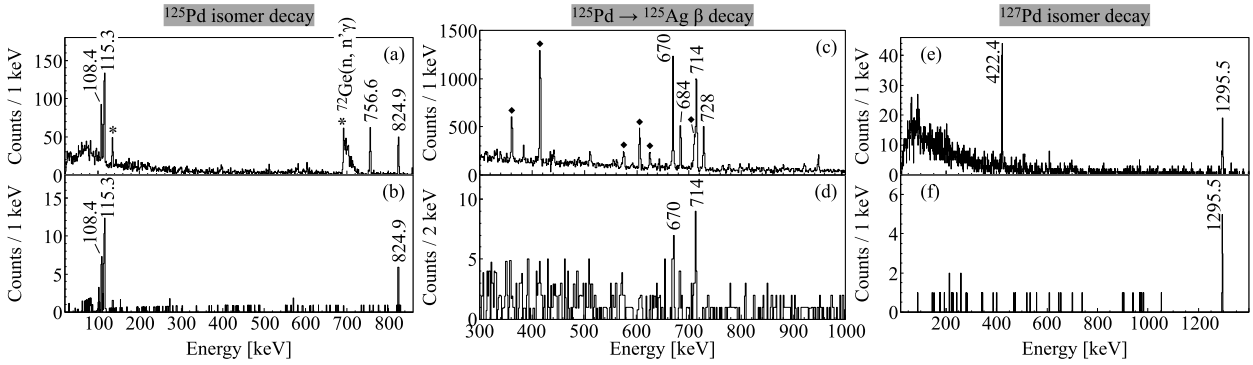

Fig. 1. Gamma-ray energy spectra measured in the present work. The coincidence gate conditions are as follows. (a) and (b): Within a time range of 250 – 1250 ns after implantation of ^{125}Pd ions. Contaminants are marked with asterisks. An additional gate is set on the 757-keV γ ray to make the coincidence spectrum shown in the panel (b). (c) and (d): Within a time interval of 0 – 200 ms following implantation of ^{125}Pd ions correlated with β rays. Long-lived activities have been subtracted. In the panel (c), γ rays assigned previously in the decay scheme from an isomeric state at 1501 keV towards the $(9/2^+)$ state in ^{125}Ag [19,20] are labeled with their energy values, while transitions reported as feeding the $(1/2^-)$ state [21] are marked with diamonds. The coincidence spectrum shown in the panel (d) is obtained with a sum of additional gates on the 108-, 115-, 757-, and 825-keV γ rays, which are observed within a 900-ns time window opened 100 ns after the ion implantation. (e) and (f): Within a time range of 0.25 – 100 µs after implantation of ^{127}Pd ions. An additional gate is set on the 422-keV γ ray to make the coincidence spectrum shown in the panel (f).

Table 1
Summary of transitions from the isomeric states in ^{125}Pd and ^{127}Pd. Each column shows the initial level energy E_i, spin and parity of the initial (final) state J_i^π (J_f^π), γ-ray energy E_γ, electromagnetic transition multipolarity $\sigma\lambda$, total conversion coefficient $\alpha_T^{\rm cal}$ calculated by the BrIcc code [22], relative γ-ray intensity I_γ, total transition intensity $I_{\rm tot} = (1+\alpha_T^{\rm cal})I_\gamma$, and half-life $T_{1/2}$ derived from a fit to the γ-ray time distribution.

Nucleus	E_i[a] [keV]	$J_i^\pi \rightarrow J_f^\pi$	E_γ [keV]	$\sigma\lambda$	$\alpha_T^{\rm cal}$	I_γ[b] [relative]	$I_{\rm tot}$ [relative]	$T_{1/2}(\gamma)$
$^{125}Pd_{79}$	1805.2	$(23/2^+) \rightarrow (19/2^+)$	108.4(1)	$E2$	1.05	48(6)	99(13)	138(11) ns
	1696.8	$(19/2^+) \rightarrow (19/2^-)$	115.32(6)	$E1$	1.02×10^{-1}	100(11)	110(12)	151(9) ns
	756.6	$(15/2^-) \rightarrow (11/2^-)$	756.56(9)	$E2$	1.95×10^{-3}	100(11)	100(11)	153(7) ns
	1581.5	$(19/2^-) \rightarrow (15/2^-)$	824.94(9)	$E2$	1.58×10^{-3}	93(11)	93(11)	134(7) ns
$^{127}Pd_{81}$	1717.9	$(19/2^+) \rightarrow (15/2^-)$	422.4(1)	$M2$	3.01×10^{-2}	100(21)	103(21)	41(8) µs
	1295.5	$(15/2^-) \rightarrow (11/2^-)$	1295.5(2)	$E2$	6.00×10^{-4}	105(24)	105(24)	36(9) µs

[a] Relative to the respective $(11/2^-)$ states.
[b] Relative to the 757-, and 422-keV γ-ray intensities for ^{125}Pd and ^{127}Pd, respectively.

the $11/2^-$ state is likely to feed $J = 9/2$, 11/2, and 13/2 levels in the daughter nucleus, while comparatively low-spin states can be populated in the β decay from the $3/2^+$ state. As an example of the ^{125}Pd → ^{125}Ag decay, a β-delayed γ-ray spectrum measured within 200 ms after implantation of the ^{125}Pd ions is shown in Fig. 1(c). The 670-, 684-, 714-, and 728-keV γ rays, which were reported previously as the transitions involved in the cascade sequences from the $(17/2^-)$ isomer at 1501 keV to the presumed $(9/2^+)$ ground state in ^{125}Ag [19,20], are unambiguously observed, supporting the presence of the $(11/2^-)$ state in ^{125}Pd that undergoes β decay to ^{125}Ag. In addition to these known transitions, it was found that several new γ rays emerge, being assigned as feeding the low-spin states in ^{125}Ag. Further details of the β-γ analysis will be presented elsewhere [21].

In order to clarify on which β-decaying state ($J^\pi = 3/2^+$ or $11/2^-$) the aforementioned 144-ns isomer is built in ^{125}Pd, the correlation between the β-delayed γ rays and the preceding isomeric-decay transitions has been confirmed. Fig. 1(d) shows a γ-ray energy spectrum created under the same gate condition for the implant-β-γ correlation as that used for Fig. 1(c), and additionally, with a sum of energy gates on the 108-, 115-, 757-, and 825-keV γ rays observed within a 0.1 – 1.0 µs time interval after implantation of the ^{125}Pd ions. With this constraint on the "isomer implantation" events, it is expected that delayed γ rays following the β decay from the state to which the 144-ns isomer finally decays can be enhanced, compared to the transitions populated from the other β-decaying state. It can be seen in Fig. 1(d) that γ-ray peaks at 670 and 714 keV, which were previously assigned as the $(11/2^+) \rightarrow (9/2^+)$ and $(13/2^+) \rightarrow (9/2^+)$ transitions in ^{125}Ag, respectively [19,20], are clearly visible, while the other γ rays reduce their peak counts as low as the background fluctuations. Therefore, the 144-ns isomer turned out to be built on the β-decaying state with $J^\pi = (11/2^-)$ in ^{125}Pd, though it is still unclear whether this level is the ground state or the long-lived isomer from the present experimental result. Note that whichever the $(11/2^-)$ level is, the ground state or the long-lived isomer, the discussions and conclusions regarding higher-lying levels presented below are not changed. The excitation energy of the 144-ns isomer was determined to be 1805 keV relative to the $(11/2^-)$ state.

The level scheme of ^{125}Pd established in the present work is exhibited in Fig. 3 (left). The order of the 757- and 825-keV cascade transitions was determined in comparison with the 693-keV $[(2^+) \rightarrow 0^+]$ and 788-keV $[(4^+) \rightarrow (2^+)]$ transitions in the neighboring $N = 80$ isotope ^{126}Pd [11]. However, the possibility of inversion of these transitions can not be entirely ruled out due to the closeness of their energies. The levels at 757 (or 825) and 1582 keV relative to the $(11/2^-)$ state were tentatively assigned spins and parities of $15/2^-$ and $19/2^-$, respectively, which are interpreted as a neutron (hole) in the $h_{11/2}$ orbital coupled to the (2^+) and (4^+) states in ^{126}Pd. Meanwhile, the $15/2^+$ assignment for the 1582-keV state, the analog of the one observed in the $N = 79$ isotone ^{129}Sn [25], can be ruled out because of the absence of a competing $E1$ branch towards a (presumed) $13/2^-$ state, which arises predominantly from the $\nu h_{11/2}^{-1} \otimes 2^+$ multiplet, and therefore, is expected to appear in the proximity of the $(15/2^-)$ state.

The transitions of 108 and 115 keV are placed in cascade above the 1582-keV level. For the 108-keV transition, a total internal conversion coefficient α_T of 1.1(3) can be deduced from its γ-ray intensity being compared to the total intensity of the 757-keV, $E2$ transition, see Table 1. This α_T value is in good agreement with the

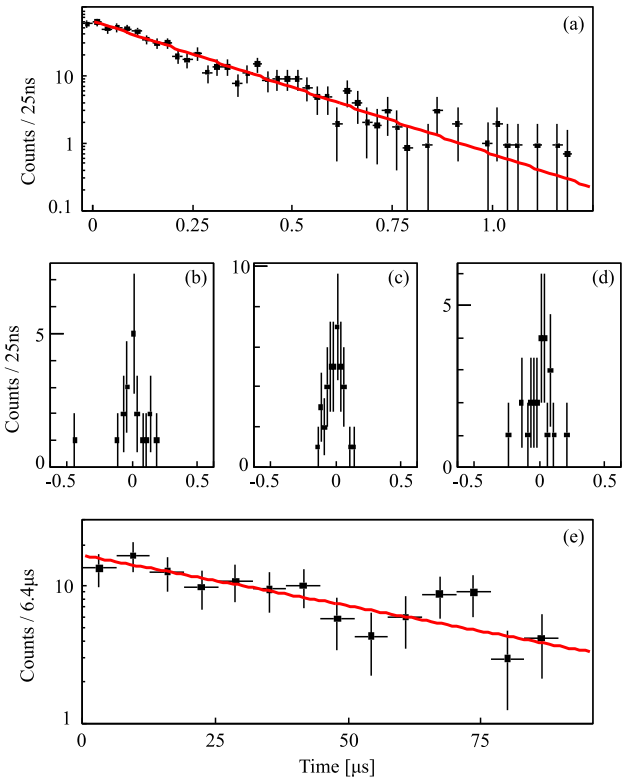

Fig. 2. (a): Time spectrum (t_γ) of the 757-keV γ ray in ^{125}Pd. (b): Time difference spectrum ($\Delta t_{\gamma\gamma}$) of the 115-keV γ ray relative to the 108-keV transition in ^{125}Pd. (c) and (d): Sum of $\Delta t_{\gamma\gamma}$ of the 757- and 825-keV γ rays relative to the 115- and 108-keV transitions in ^{125}Pd, respectively. (e): t_γ of the 422-keV γ ray in ^{127}Pd. In the panels (a) and (e), the red solid lines represent the results of a log-likelihood fit.

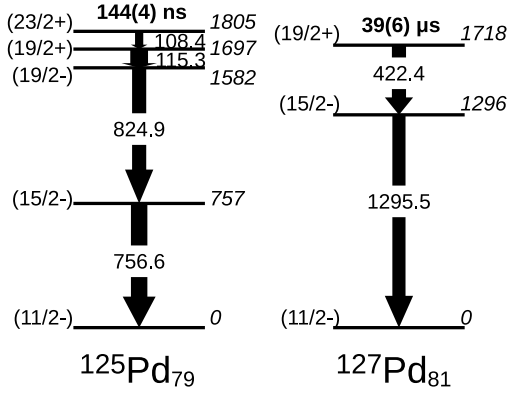

Fig. 3. Level schemes of ^{125}Pd and ^{127}Pd established in the present work. Each level is labeled with the spin-parity (J^π) and energy (relative to the $11/2^-$ state) values. The measured (isomeric) half-lives are indicated in bold. The widths of solid arrows are proportional to the γ-ray relative intensities summarized in Table 1.

theoretical value of 1.05 for an $E2$ multipolarity [22]. Similarly, the value obtained from the intensity balance analysis for the 115-keV transition, $\alpha_T = 0.0(1)$, is consistent only with an $E1$ multipolarity within the margin of error. The ordering of these transitions was determined based on the arguments on transition strengths. If the 108-keV ($E2$) transition were placed below the 115-keV ($E1$) transition, an intermediate state presumed at 1690 keV should have a half-life of the order of a few or several hundreds of nanoseconds [e.g. $T_{1/2} \approx 500$ ns given the reduced transition probability $B(E2) = 1$ W.u. for the 108-keV transition]. This is at variance with what was observed from time difference spectra having almost symmetric distributions, as shown in Figs. 2(b), 2(c), and 2(d). Therefore, we conclude that the 108-keV transition deexcites the 144-ns isomer at 1805 keV relative to the $(11/2^-)$ state, followed by the 115-keV transition that feeds the 1582-keV level. It is to be noted that the measurement of the prompt relative-time distributions shown in Figs. 2(b), 2(c), and 2(d) also indicates that neither the (intermediate) 1697-keV state nor the 1582-keV state is isomeric, supporting the $19/2^-$ assignment for the latter level, and accordingly, excluding the possibility of $19/2^+$ analogous to the one identified as the 17.5- μs isomer in the $N = 79$ isotone ^{127}Cd [26].

Based on the above arguments on intensity balances and transition strengths, either a spin-parity assignment of $23/2^+ \rightarrow 19/2^+ \rightarrow 19/2^-$ or $25/2^+ \rightarrow 21/2^+ \rightarrow 19/2^-$ can be proposed for the $108-115$-keV cascade between the 144-ns isomer and the 1582-keV state in ^{125}Pd. In the following discussion, the former sequence is adopted with the help of shell-model calculations. The reduced transition probability, $B(E2) = 129(4)$ e^{2}fm^4 $= 3.47(9)$ W.u., can be obtained for the 108-keV transition from the measured half-life of the 1805-keV isomeric state, taking into account the internal conversion process with the calculated α_T value [22]. This $B(E2)$ value is comparable to the corresponding $23/2^+ \rightarrow 19/2^+$ transition observed in the $N = 79$ isotone ^{129}Sn [25].

For ^{127}Pd, two γ-ray peaks at 422 and 1296 keV have been prominently observed within a long time window ranging from 0.25 to 100 μs after the ion implantation, and their coincidence relationship confirmed by γ-γ coincidence analyses, see Figs. 1(e) and 1(f). The isomeric half-life was determined to be 39(6) μs from a weighted average of the respective fits to the time distributions of the 422- and 1296-keV γ rays, the former of which is shown in Fig. 2(e) as an exemplary case.

The level scheme of ^{127}Pd is proposed as exhibited in Fig. 3 (right). The 39- μs isomeric state has been identified at an excitation energy of 1718 keV with respect to the $(11/2^-)$ level, which is assumed to be the lowest-lying state in the isomeric-decay cascade in analogy with ^{125}Pd. The 1296-keV transition was assigned as feeding the $(11/2^-)$ state from the $(15/2^-)$ level owing to a close resemblance of the energy to the $(2^+) \rightarrow 0^+$ transition (1311 keV) in the neighboring $N = 82$ nucleus ^{128}Pd [10]. Concerning the 422-keV transition that de-excites the isomeric state, $E3$ and higher-multipole possibilities can be virtually ruled out because their strengths would be unlikely enhanced compared to the transitions known in this region (see Table 2 in Ref. [18]). Meanwhile, a single de-excitation of 422 keV with an $E1$, $M1$, or $E2$ multipolarity would not result in such a long-lived isomeric state. Consequently, the 422-keV transition is expected to have $M2$ character with a reduced transition probability of $9.6(15) \times 10^{-2}$ μ_N^2fm^2 $= 2.3(4) \times 10^{-3}$ W.u., which is emitted from the $(19/2^+)$ isomeric state to the $(15/2^-)$ state.

Here, it is to be noted that the possible existence of a low-energy (unobserved) transition above the 1718-keV level as de-exciting the 39- μs isomeric state can be excluded for the following reasons: In this scenario, the presumed *non-isomeric* state at 1718 keV is expected to have $19/2^-$, which decays to the $(15/2^-)$ state at 1296 keV via an $E2$ transition, similar to the decay sequence observed for ^{125}Pd. Assuming an observation limit of 20 counts for an expected γ-ray peak in the ion-γ correlated spectrum shown in Fig. 1(e), depending on conversion, limits on the transition energy can be determined for different multipolarities λ. Regardless of the transition energy, the 39- μs isomeric-decay transition is unlikely to proceed with $\lambda \geq 3$ and $\lambda = 1$ on account of the same reason as the one concerning the transition strengths discussed in the previous paragraph. Provided that the unobserved transition has $M2$ multipolarity, the transition energy would have to be lower than 90 keV with the reduced transition probability of the order of 1

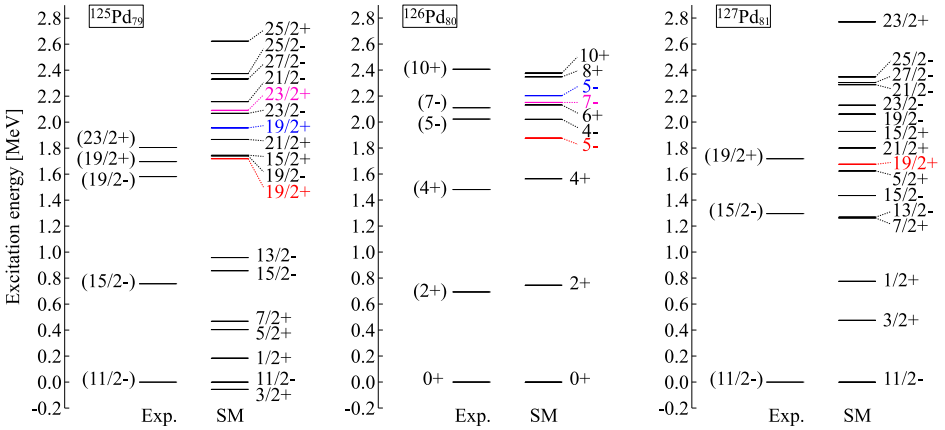

Fig. 4. Comparison between experimental and calculated level energies in neutron-rich Pd isotopes. The experimental values for the ^{126}Pd levels are taken from Refs. [10,11], while those for ^{125,127}Pd are from the present work. SM represents a shell-model calculation performed with considering a neutron cross-shell excitation (see text).

Table 2
Experimental and theoretical $B(\sigma\lambda)$ values for the selected transitions in ^{A}Pd isotopes.

A	Transition	$\sigma\lambda$	$B(\sigma\lambda)$ [W.u.]	
			Exp.	SM
125	$23/2^+ \to 19/2^+_2$	$E2$	3.47(9)	5.2
	$23/2^+ \to 19/2^+_1$	$E2$	–	1.1×10^{-7}
126	$7^- \to 5^-_2$	$E2$	2.13(14)	5.7
	$7^- \to 5^-_1$	$E2$	–	3.9×10^{-9}
127	$19/2^+ \to 15/2^-$	$M2$	$2.3(4) \times 10^{-3}$	7.6×10^{-3}

W.u. or larger. Such an unhindered $M2$ transition, which exceeds a recommended upper limit of the transition strength [27], hardly occurs in the region of interest. If the isomeric decay is of $E2$ character from a $23/2^-$ state, an upper limit of the transition energy would be 75 keV for it not to have been observed. For such a low-energy transition, the $B(E2)$ value from the 39- μs isomeric state is estimated to be in the order of $0.01 - 0.1$ W.u., which could be possible as observed for the $(8^+) \to (6^+)$ isomeric transition in ^{128}Pd [10]. However, if a $23/2^-$ state were isomeric, it would prefer to decay via a fast $E1$ transition to a lower-lying $21/2^+$ level, which is predicted by a shell-model calculation as will be discussed later, rather than the nearby $19/2^-$ state. Thus, the possibility of a low-energy isomeric-decay transition can be ruled out for any multipolarities, supporting the $(19/2^+)$ assignment for the 39- μs isomeric state at 1718 keV relative to the $(11/2^-)$ level.

In order to understand systematically the level properties of the neutron-rich Pd isotopes towards $N = 82$, shell-model calculations based on the extended pairing plus quadrupole-quadrupole forces combined with monopole corrections (EPQQM) [28] have been performed for ^{125,126,127}Pd. With the doubly magic nucleus ^{78}Ni as the closed core, the model space considered includes four orbits in the $Z = 28 - 50$ major shell and the $g_{7/2}$, $d_{5/2}$ orbits above the $Z = 50$ shell gap for protons, and five orbits in the $N = 50 - 82$ major shell and the $f_{7/2}$, $p_{3/2}$ orbits above the $N = 82$ shell gap for neutrons. The proton/neutron single-particle energies, effective charges and g-factors, and the parameters of the EPQQM Hamiltonian employed in the present calculations are consistent with those adopted in the previous works [29–32]. The observed and calculated level energies are compared in Fig. 4, where the columns marked with SM exhibit the results of a large-scale shell model that allows the excitation of a neutron across the shell gap of $N = 82$. The measured and calculated values of the reduced transition probabilities for the selected transitions are summarized in Table 2.

As mentioned earlier, experimentally there remains a possible spin-parity assignment of $23/2^+ \to 19/2^+$ or $25/2^+ \to 21/2^+$ for the 108-keV transition deexciting the isomeric state in ^{125}Pd. However, the yrast $25/2^+$ level is unlikely to be isomeric in comparison with the shell-model calculation, which predicts that the energy difference between the $25/2^+$ and $21/2^+$ states is much larger than the observed transition energy, as shown in Fig. 4. Consequently, the excited states at 1697 and 1805 keV in ^{125}Pd are assigned spins and parities of $(19/2^+)$ and $(23/2^+)$, respectively.

For the higher-lying levels in ^{125}Pd, the shell-model calculation predicts that there are two $19/2^+$ states below an excitation energy of 2 MeV, as indicated with different colors in Fig. 4. The first $19/2^+$ (hereinafter denoted by $19/2^+_1$) state is predicted to involve predominantly a two-proton-hole excitation $\pi(g^{-1}_{9/2}p^{-1}_{1/2})$ together with an inactive proton-hole pair $\pi(g^{-2}_{9/2})_{0^+}$, coupled to an active neutron hole in the $h_{11/2}$ orbit (and a neutron-hole pair coupled to spin zero). Meanwhile, the $19/2^+_2$ state is dominated by neutron-hole excitations of the type $(\nu^{-3})_{19/2^+}$, such as $\nu(h^{-2}_{11/2}d^{-1}_{3/2})$, $\nu(h^{-2}_{11/2}s^{-1}_{1/2})$, and $\nu(h^{-2}_{11/2}g^{-1}_{7/2})$, coupled to an inactive proton component, $\pi(g^{-4}_{9/2})_{0^+}$ or $\pi(g^{-2}_{9/2}p^{-2}_{1/2})_{0^+}$. Thus, the proton and neutron excitations within the respective major shells are suggested to compete with each other in ^{125}Pd.

According to the present shell-model calculation for ^{125}Pd, the major components of the $23/2^+$ wave function differ significantly from those of the $19/2^+_1$ state, resulting in a strongly hindered $E2$ transition, see Table 2. On the other hand, very similar wave functions are predicted for the $23/2^+$ and $19/2^+_2$ states of ^{125}Pd. The fact that the measured $B(E2)$ value for the isomeric deexcitation is fairly consistent with the calculated $B(E2; 23/2^+ \to 19/2^+_2)$ value indicates that both the experimental $(23/2^+)$ and $(19/2^+)$ levels are dominated by the neutron excitations, as argued in the last paragraph. A candidate for the $19/2^+_1$ shell-model state, which is dominated by the proton excitations, has not been identified in the current experiment.

Similar decay patterns are suggested to take place in the one-neutron neighbor ^{126}Pd. As compared in Table 2, the experimental $B(E2)$ value for the $(7^-) \to (5^-)$ transition [10] is well reproduced by SM given the $E2$ transition towards the 5^-_2 level, thus suggesting that the calculated 5^-_2 level corresponds to the (5^-) state observed at 2023 keV [10]. In contrast, the $7^- \to 5^-_1$ deexcitation is calculated to be extremely hindered, similar to the aforementioned $23/2^+ \to 19/2^+_1$ transition in ^{125}Pd. Analyzing the shell-model wave functions, it can be found that the main configurations of the $5^-_{1,2}$ and 7^- states in ^{126}Pd are almost equivalent to

the $19/2^+_{1,2}$ and $23/2^+$ states in ^{125}Pd, respectively, with the addition of a neutron in the $h_{11/2}$ orbit, i.e., the proton excitations and neutron excitations respectively dominate the 5^-_1 level and the 5^-_2, 7^- levels.

The excitation spectra and the reduced transition probability for the $(19/2^+) \rightarrow (15/2^-)$, $M2$ decay observed for ^{127}Pd are reproduced satisfactorily by the shell-model calculation. The $19/2^+$ state is predicted to have a wave function with the leading component, $\pi(g^{-3}_{9/2}p^{-1}_{1/2}) \otimes \nu(h^{-1}_{11/2})$, the analog of the $19/2^+_1$ state in ^{125}Pd. Note that the current shell model predicts a $21/2^+$ state, which corresponds to the 3.6-ms isomer identified in the $N = 81$ isotone ^{129}Cd [33], to be slightly higher in energy than the $19/2^+$ level, see Fig. 4. The $21/2^+$ shell-model state has almost the same configuration as the $19/2^+$ isomeric state in ^{127}Pd. The wave function of the $15/2^-$ state, to which the $19/2^+$ isomer decays, consists predominantly of the $\pi(g^{-4}_{9/2}) \otimes \nu(h^{-1}_{11/2})$ component. Hence, an $M2$ decay can not proceed between their main configurations. Within the $Z = 28 - 50$ major shell, an $M2$ decay can take place through the $\pi f_{5/2} \rightarrow \pi g_{9/2}$ transition. It is therefore expected that the large hindrance of the order of 10^{-3} W.u. (see Table 2) is ascribed to the small admixture of the $\pi(g^{-3}_{9/2}f^{-1}_{5/2}) \otimes \nu(h^{-1}_{11/2})$ component in the $19/2^+$ isomeric state.

It is worth mentioning finally about the evolution of single-particle levels in this neutron-rich region and its impact on the $N = 82$ shell closure, which is also crucial for a better understanding of the r-process nucleosynthesis [13,14]. In Ref. [31], large-scale shell-model calculations, which have been done in the same framework as that adopted in the present work, suggested that the size of the $N = 82$ shell gap decreases gradually with decreasing proton number from 48 (^{130}Cd) to 36 (^{118}Kr) on account of the dynamic effect of the monopole interaction between the $\pi g_{9/2}$ and $\nu h_{11/2}$ orbitals. Since the ^{125,127}Pd states discussed above consist of these high-j orbits, the experimental results obtained in this work can serve as a stringent benchmark for testing shell models to foresee a possible $N = 82$ shell quenching in exotic nuclei, which are still inaccessible for spectroscopic study.

To conclude, spectroscopic studies of ^{125}Pd and ^{127}Pd have been performed at RIBF, and accordingly, we have provided for the first time experimental information on the excited level structure of these neutron-rich nuclei, which have triple- and single-neutron vacancies relative to the $N = 82$ closed-shell nucleus ^{128}Pd. In ^{125}Pd, a previously unreported isomeric state with a half-life of 144(4) ns was assigned tentatively a spin and parity of $23/2^+$ based on the results of the γ-ray intensity balance analysis and the measured transition strengths with the aid of a shell-model calculation. This isomer and the lower-lying $(19/2^+)$ states were interpreted as being ascribed predominantly to three-neutron-hole excitations within the $N = 50 - 82$ major shell. Meanwhile, the $(19/2^+)$ isomer identified with $T_{1/2} = 39(6)$ μs in ^{127}Pd was expected to involve the proton-hole excitation $\pi(g^{-3}_{9/2}p^{-1}_{1/2})$ coupled to a neutron hole in the $h_{11/2}$ orbit. Thus, it turned out that the $(19/2^+)$ states observed at almost the same excitation energy in ^{125}Pd and ^{127}Pd are quite different in nature. A future experimental challenge is to corroborate the argument on the different isomerism of these states by measuring nuclear magnetic moments using more intense radioactive-isotope beams.

We thank the staff at RIBF for providing the beams, the EUROBALL Owners Committee for the loan of germanium detectors, the PreSpec Collaboration for the use of the readout electronics. Part of the WAS3ABi was supported by the Rare Isotope Science Project which is funded by MSIP and NRF of Korea. This work was supported by the Priority Centers Research Program in Korea (2009-0093817), OTKA contract number K100835, the U.S. DOE, Office of Nuclear Physics (Contract No. DE-AC02-06CH11357), NRF-2016R1A5A1013277 and NRF-2013M7A1A1075764, the Spanish Ministerio de Economía y Competitividad under contract FPA2017-84756-C4-2-P, the European Commission through the Marie Curie Actions call FP7-PEOPLE-2011-IEF (Contract No. 300096), German BMBF under Contract No: 05P12PKFNE, JSPS KAKENHI Grant No. 24740188 and 25247045, the National Natural Science Foundation of China (Nos. 11505302, 11575112), the National Key Program for S&T Research and Development (No. 2016YFA0400501), and STFC (UK).

References

[1] T. Otsuka, et al., Phys. Rev. Lett. 95 (2005) 232502.
[2] T. Otsuka, Y. Tsunoda, J. Phys. G, Nucl. Part. Phys. 43 (2016) 024009.
[3] O. Sorlin, M.-G. Porquet, Prog. Part. Nucl. Phys. 61 (2008) 602.
[4] Y. Yano, Nucl. Instrum. Methods Phys. Res. B 261 (2007) 1009.
[5] T. Nakamura, H. Sakurai, H. Watanabe, Prog. Part. Nucl. Phys. 97 (2017) 53.
[6] T. Ohnishi, et al., J. Phys. Soc. Jpn. 77 (2008) 083201.
[7] T. Ohnishi, et al., J. Phys. Soc. Jpn. 79 (2010) 073201.
[8] Y. Shimizu, et al., J. Phys. Soc. Jpn. 87 (2018) 014203.
[9] G. Lorusso, et al., Phys. Rev. Lett. 114 (2015) 192501.
[10] H. Watanabe, et al., Phys. Rev. Lett. 111 (2013) 152501.
[11] H. Watanabe, et al., Phys. Rev. Lett. 113 (2014) 042502.
[12] H. Wang, et al., Phys. Rev. C 88 (2013) 054318.
[13] E.M. Burbidge, et al., Rev. Mod. Phys. 29 (1957) 547.
[14] K.L. Kratz, et al., Eur. Phys. J. A 25 (2005) 633.
[15] T. Kubo, et al., Prog. Theor. Exp. Phys. 2012 (2012) 03C003.
[16] S. Nishimura, Prog. Theor. Exp. Phys. 2012 (2012) 03C006.
[17] P.-A. Söderström, et al., Nucl. Instrum. Methods B 317 (2013) 649.
[18] H. Watanabe, Eur. Phys. J. A 55 (2019) 19.
[19] D. Kameda, et al., Phys. Rev. C 86 (2012) 054319.
[20] S. Lalkovski, et al., Phys. Rev. C 87 (2013) 034308.
[21] Z. Chen, submitted for publication.
[22] T. Kibédi, et al., Nucl. Instrum. Methods A 589 (2008) 202.
[23] http://www.nndc.bnl.gov/ensdf/.
[24] D.T. Yordanov, et al., Phys. Rev. Lett. 110 (2013) 192501.
[25] R.L. Lozeva, et al., Phys. Rev. C 77 (2008) 064313.
[26] F. Naqvi, et al., Phys. Rev. C 82 (2010) 034323.
[27] P. Endt, At. Data Nucl. Data Tables 26 (1981) 47.
[28] M. Hasegawa, K. Kaneko, Phys. Rev. C 59 (1999) 1449–1455.
[29] H.-K. Wang, et al., Phys. Rev. C 88 (2013) 054310.
[30] H.-K. Wang, K. Kaneko, Y. Sun, Phys. Rev. C 89 (2014) 064311.
[31] H.-K. Wang, K. Kaneko, Y. Sun, Phys. Rev. C 91 (2015) 021303.
[32] H.-K. Wang, et al., Phys. Rev. C 95 (2017) 011304.
[33] J. Taprogge, et al., Phys. Lett. B 738 (2014) 223.